IOP PUBLISHING CLASSICAL AND QUANTUM GRAVITY

Class. Quantum Grav. **24** (2007) S671–S679 doi:10.1088/0264-9381/24/19/S29

Gravitational waves by gamma-ray bursts and the Virgo detector: the case of GRB 050915a

F Acernese[1], P Amico[2], M Alshourbagy[3], F Antonucci[4], S Aoudia[5], P Astone[4], S Avino[1], D Babusci[6], G Ballardin[7], F Barone[1], L Barsotti[3], M Barsuglia[8], Th S Bauer[9], F Beauville[10], S Bigotta[3], S Birindelli[3], M A Bizouard[8], C Boccara[11], F Bondu[5], L Bosi[2], C Bradaschia[3], S Braccini[3], F J van den Brand[9], A Brillet[5], V Brisson[8], D Buskulic[10], E Calloni[1], E Campagna[12], F Carbognani[7], F Cavalier[8], R Cavalieri[7], G Cella[3], E Cesarini[12], E Chassande-Mottin[5], N Christensen[7], C Corda[3], A Corsi[4], F Cottone[2], A-C Clapson[8], F Cleva[5], J-P Coulon[5], E Cuoco[7], A Dari[2], V Dattilo[7], M Davier[8], M del Prete[3], R De Rosa[1], L Di Fiore[1], A Di Virgilio[3], B Dujardin[5], A Eleuteri[1], M Evans[7], I Ferrante[3], F Fidecaro[3], I Fiori[7], R Flaminio[7,10], J-D Fournier[5], S Frasca[4], F Frasconi[3], L Gammaitoni[2], F Garufi[1], E Genin[7], A Gennai[3], A Giazotto[3], G Giordano[6], L Giordano[1], R Gouaty[10], D Grosjean[10], G Guidi[10], S Hamdani[7], S Hebri[7], H Heitmann[5], P Hello[8], D Huet[7], S Karkar[10], S Kreckelbergh[8], P La Penna[7], M Laval[5], N Leroy[8], N Letendre[10], B Lopez[7], M Lorenzini[12], V Loriette[11], G Losurdo[12], J-M Mackowski[13], E Majorana[4], C N Man[5], M Mantovani[3], F Marchesoni[2], F Marion[10], J Marque[7], F Martelli[12], A Masserot[10], M Mazzoni[12], L Milano[1], F Menzinger[7], C Moins[7], J Moreau[11], N Morgado[13], B Mours[10], F Nocera[7], C Palomba[4], F Paoletti[3,7], S Pardi[1], A Pasqualetti[7], R Passaquieti[3], D Passuello[3], F Piergiovanni[12], L Pinard[13], R Poggiani[3], M Punturo[2], P Puppo[4], S van der Putten[9], K Qipiani[1], P Rapagnani[4], V Reita[11], A Remillieux[13], F Ricci[4], I Ricciardi[1], P Ruggi[7], G Russo[1], S Solimeno[1], A Spallicci[5], M Tarallo[3], M Tonelli[3], A Toncelli[3], E Tournefier[10], F Travasso[2], C Tremola[3], G Vajente[3], D Verkindt[10], F Vetrano[12], A Viceré[12], J-Y Vinet[5], H Vocca[2] and M Yvert[10]

[1] INFN, sezione di Napoli and/or Università di Napoli 'Federico II' Complesso Universitario di Monte S.Angelo, and/or Università di Salerno, Fisciano (Sa), Italy
[2] INFN, Sezione di Perugia and/or Università di Perugia, Perugia, Italy
[3] INFN, Sezione di Pisa and/or Università di Pisa, Pisa, Italy
[4] INFN, Sezione di Roma and/or Università 'La Sapienza', Roma, Italy
[5] Departement Artemis—Observatoire de la Côte d'Azur, BP 42209 06304 Nice, Cedex 4, France
[6] INFN, Laboratori Nazionali di Frascati, Frascati (Rm), Italy
[7] European Gravitational Observatory (EGO), Cascina (Pi), Italy
[8] LAL, Univ Paris-Sud, IN2P3/CNRS, Orsay, France
[9] NIKHEF, NL-1009 DB Amsterdam and/or Vrije Universiteit, NL-1081 HV Amsterdam, The Netherlands
[10] Laboratoire d'Annecy-le-Vieux de Physique des Particules (LAPP), IN2P3/CNRS, Université de Savoie, Annecy-le-Vieux, France
[11] ESPCI, Paris, France
[12] INFN, Sezione di Firenze/Urbino, Sesto Fiorentino, and/or Università di Firenze, and/or Università di Urbino, Italy
[13] LMA, Villeurbanne, Lyon, France

E-mail: Alessandra.Corsi@iasf-roma.inaf.it

Received 13 April 2007, in final form 8 August 2007
Published 19 September 2007
Online at stacks.iop.org/CQG/24/S671

Abstract
In the framework of the expected association between gamma-ray bursts and gravitational wave signals, we present the preliminary results of an analysis aimed to search for bursts of gravitational waves associated with the long GRB 050915a. GRB 050915a was detected by the Swift satellite in 2005, when the Virgo detector was engaged in one of its science runs, namely the C7 run, during which the best sensitivity attained in 2005 was exhibited. This offered the opportunity for the first coincident analysis between a gamma-ray burst and the Virgo gravitational wave detector. Here we give an overview of this ongoing analysis, which at the end will play the role of a prototype, crucial in defining a methodology for gamma-ray burst triggered searches with Virgo. The final results of our analysis will also allow us to evaluate up to which level Virgo will be able to constrain the amplitude of the gravitational wave signal from a typical long gamma-ray burst.

PACS numbers: 95.55.Ym, 95.85.Sz, 97.60.−s, 98.70.Rz

1. Introduction

Gamma-ray bursts (GRBs) are among the most luminous sources in the Universe. They are characterized by an intense emission of γ-ray (and x-ray) photons, corresponding to an isotropic energy release of the order of 1 $M_{\odot}c^2$, on timescales of the order of seconds. The observed bimodal distribution of GRB durations allowed us to discriminate between *long* bursts, typically lasting longer than 2 s, and *short* bursts, shorter than 2 s. The sudden burst of γ-ray photons is followed by a multi-wavelength (radio-to-x-rays) emission called 'afterglow', discovered by the Italian–Dutch satellite BeppoSAX in 1997 [1]. The BeppoSAX discovery regarded long GRBs. The afterglow of short GRBs was localized for the first time only recently, by the *Swift* satellite [2]. The discovery of the optical afterglow [3] has opened the way to the identification of host galaxies and to redshift measurements. Performed by identifying absorption lines in the spectrum of the optical afterglow (caused by the gas in the GRB host galaxy), or by measuring the host emission lines at late times, redshift measurements have confirmed the cosmological origin of GRBs. The smallest observed redshift is $z = 0.0085$ (i.e. a luminosity distance $d_L \simeq 40$ Mpc), for the long GRB 980425 [4].

GRBs are likely associated with a catastrophic energy release in stellar mass objects. The sudden emission of a large amount of energy in a compact volume leads to the formation of a 'fireball' of $e^{\pm}$ pairs, γ-rays and baryons, while a fraction of the liberated energy is converted into gravitational waves (GWs). Currently, the leading model for the electromagnetic signal is the so-called 'fireball model' [5–8]. In this model, the electromagnetic emission is the result of kinetic energy dissipation within the fireball, where shocks accelerate electrons that radiate via synchrotron emission.

Since the electromagnetic signal is emitted at distances greater than $\sim 10^{13}$ cm from the GRB source, the central engine is hidden from direct observation in the electromagnetic window. Nonetheless, these observations provided significant constraints on the engines producing these energetic explosions (see, e.g., [9–11]). Currently, the mostly favored progenitor scenarios are compact binary coalescence, for short bursts, and death of massive stars, for long bursts [6]. A direct signature of the progenitor's identity may come from GWs. The fraction of energy that is expected to be radiated in GWs during the catastrophic event leading to a GRB would, in fact, come from the immediate neighborhood of the GRB source.

At the time of GRB 050915a, Virgo was engaged in the 5-day data run C7. The Virgo detector was still undergoing commissioning, but its sensitivity during C7 exceeded that of any previous run. The lowest strain noise was $\sim 6 \times 10^{-22}$ Hz$^{-1/2}$ around $\sim$300 Hz. An analysis of Virgo data simultaneous with the long GRB 050915a is currently being performed, aimed to search for a possible short burst of GWs associated with this GRB. Based on current theoretical estimates (e.g. [12]) and on the typical distance of long GRBs (the redshift of this burst is not known, but the mean redshift in the *Swift* sample is $z > 2$ [13]), we expect the searched signal in the Virgo detector to be very weak, below the detector noise [12]. In the absence of a detection, this analysis will set an upper limit on the strength of the GW emission.

In what follows, we give an overview of the ongoing analysis of Virgo data (see also [14]). A more detailed description of the analysis and the presentation of its final results will be the subject of a forthcoming paper [15]. In section 2, we summarize the current scenario for GRB progenitors and the associated GW signal; in section 3, we briefly recall GRB 050915a detection by the *Swift* satellite; in section 4 we give an overview of our analysis; finally, in section 5 we give our conclusions.

2. Progenitor models and the expected GW signal

The energetics of GRBs, together with their rapid variability, suggest a general picture in which they arise during the accretion of a massive disk onto a compact object, most likely a newborn black hole (BH). A compact object is required by the short variability timescale observed in their γ-ray light curves, accretion is needed to produce the duration timescale, and a massive ($\sim 0.1 M_{\odot}$) disk is required because of the energetics [8].

For the class of long GRBs, the favored progenitor candidate is the collapse of a massive star [16–18]. This scenario is usually referred to as the collapsar scenario. One of the main clues that long GRBs are related to the death of massive stars comes from their association with star forming galaxies (e.g. [10, 19]), characterized by high formation rates and young stellar populations. Moreover, the collapsar scenario has received strong support after the secure detection of supernova events associated with some long GRBs [4, 20, 21].

On the other hand, short GRBs are unlikely to result from the death of massive stars, since in such a case the natural timescale, the free-fall time, is of the order of tens of seconds, significantly longer than their short durations (see, e.g., [22]). For short bursts, the most widely speculated candidates are mergers of neutron star–neutron star (NS–NS) or neutron star–black hole (NS–BH) binaries [23–31], which, losing orbital angular momentum by GW radiation, undergo a merger. Short GRB progenitor scenarios have only recently begun to be tested thanks to the *Swift* detection of short burst afterglows [22], providing the first identifications of host galaxies. The number of elliptical hosts is of significant interest for the most frequently discussed progenitor scenario of short GRBs, the merger of NS binaries, which would be relatively more abundant in old stellar population galaxies such as ellipticals. Recent observations have shown that short GRBs associated with this kind of host do exist [22].

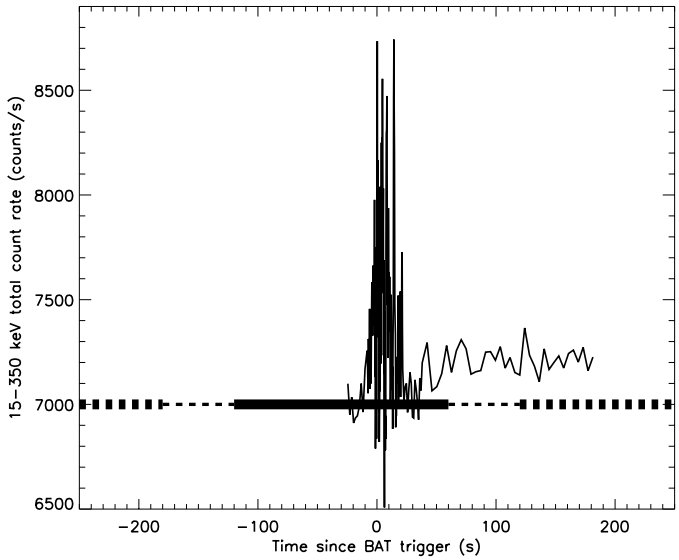

Figure 1. BAT (15-350 keV) light curve of GRB 050915a in total count rate (counts s^{-1}). BAT data of GRB 050915a has been downloaded from [40]. The time interval marked with the thick solid line defines the time length and position of the signal region. The thin-dashed segments mark the 60 s of data before the start and after the end of the signal region which are excluded from the analysis (so to separate the background from the signal). The thick-dashed segments mark the portions of the background region around the GRB trigger time. The whole background region is much longer, extending on the left of the plot up to −9973 s, and on the right of the plot up to 6872 s.

Both leading GRB progenitor candidates, stellar core collapse and merger of compact binaries, have been studied as potential sources of GWs. Estimates for their GW strain can be found, for instance, in [12]. If some fraction of GRBs are produced by NS–NS or NS–BH mergers, the GW chirp signal of the in-spiral phase should be observed. On the other hand, in long GRB progenitor scenarios, one expects GW signals arising from the ring-down phase of the newborn BH, as well as a possible contribution of a bar configuration or blob merger, generated by gravitational instability in the accretion disk and/or collapsing core [12].

The LIGO Scientific Collaboration recently published upper limit estimates for the gravitational energy released in association with the long GRB 030329 [32]. This analysis has shown that when current generation interferometric detectors will reach their nominal sensitivity, it will be possible to start constraining, for the nearest GRBs, at least the most optimistic theoretical expectations for the energy emitted in GWs (see, e.g., [33]).

3. Swift detection of GRB 050915a

On the 15th of September 2005, at 11:22:42 UT, the 'Burst Alert Telescope' (BAT) on-board *Swift* [34] triggered and located GRB 050915a [35]. The calculated position was RA = 05 h 26 m 51 s, DEC = −28 d 01′ 48″ (J2000), with an uncertainty of 3 arcmin. The BAT light curve showed a multi-peak structure, with about seven 2 s long peaks from T−10 s to T+20 s, and one more peak at about T+43 s [36]. The T_{90} duration of the burst in the 15−350 keV band was 53 ± 3 s [36], making it a long-type GRB (see figure 1). The 'X-Ray Telescope'

(XRT) began observing the BAT position at 11:24:09 UT (∼87 s after the trigger, [37]). The new refined position was RA = 05 h 26 m 44.6 s, DEC = −28 d 01′ 01″.0 (J2000) [37].

4. Search for a burst of GWs associated with GRB 050915a

The Virgo experiment is the result of an Italian–French collaboration [38]. Jointly funded by the INFN (Italy) and CNRS (France), this detector is located at the European Gravitational Observatory (EGO), near Pisa. A description of the principle of operation of Virgo and a recent review of its status can be found in [39].

At the time of GRB050915a, Virgo was collecting data in science mode, allowing for the first coincidence search between Virgo and a GRB trigger. For our analysis, we rely on a single stretch of data, between GPS times 810 808 602 s and 810 825 447 s, for a total of 16 845 s, containing the GRB trigger time (i.e. GPS time ∼810 818 575 s). We define signal region a data segment 180 s long, 120 s before the GRB trigger time and 60 s after (see the thick solid line in figure 1). This is the time window where we search for a coincidence with the GRB trigger. The rest of the data in the stretch, with the exception 60 s before the start and after the end of the signal region (see the thin-dashed lines in figure 1), belong to what we define background region (see the thick-dashed lines in figure 1). Data in this region are used to study the statistical properties of the detector noise.

Apart from the necessity of considering the trigger uncertainty, a 180 s duration for the signal region (∼3.5 times the GRB duration) is chosen to cover most of astrophysical predictions regarding the expected delay between the GRB and the associated burst-type GW signal. In the case of a collapsar (relevant for GRB 050915a), the GW burst should precede the electromagnetic trigger, with a time delay dominated by the time necessary for the fireball to push through the envelope of the GRB stellar progenitor, of the order of 10–100 s [41]. Choosing a signal region starting 120 s before the trigger time, we over-cover those predictions. Moreover, some models predict that a GW signal should be emitted during the GRB emission [33]. Considering that GRB 050915a had a T_{90} duration of 53 ± 3 s (see section 3), we have chosen our signal region to end 60 s after the trigger.

In the case of a long GRB, the associated core-collapse, BH formation and ring-down may produce a detectable GW signal. Due to the lack of accurate predictions on such a signal, we implement an analysis technique that does not rely on detailed predictions on the waveform, but only imposes general bounds on signal duration and frequency.

To search for burst-like events, we run on both the background and signal region the ‘Wavelet Detection Filter’ (WDF, see [42, 43]), a wavelet-based transient detection tool. Data are sampled at a rate of 20 kHz and no band-pass filter is applied, so that all frequencies are considered in the analysis. Before running the WDF, the raw data are whitened as described in [44]. The result of the pre-processing is a data segment with a flat power-spectral density (white noise). No vetoes or data quality cuts are applied in our analysis in order to keep the integrity of the data in the GRB window. The capability of wavelet-based algorithms in catching a signal depends on the similarities between the analyzing wavelet and the signal itself. The WDF performs a decomposition in the wavelet domain by using different wavelet basis, so as to better match different types of signal waveforms. The most popular family of orthonormal wavelets used is the Daubechies one.

The output of the WDF is a list of triggers, each characterized by a time and a signal-to-noise ratio (SNR). The filter performs the wavelet decomposition in a time window (wavelet window) 12.8 ms long, which is moved on the data at steps of 0.6 ms. At each step, a trigger is registered, its time being the initial time of the corresponding wavelet window. Events having a duration greater than 0.6 ms are thus recognized by the filter as different triggers.

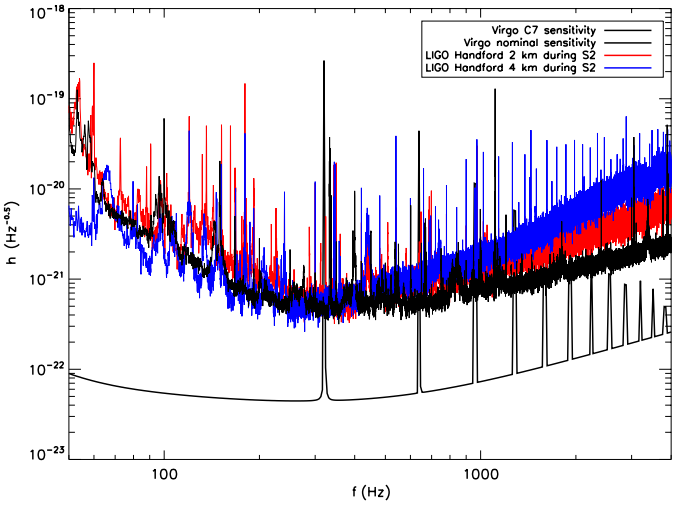

Figure 2. Virgo sensitivity during C7 run and Virgo nominal sensitivity are plotted in black. Typical LIGO Hanford sensitivities during the S2 are shown in red and blue, for the 2 km and 4 km, respectively. LIGO sensitivity curves have been downloaded from [45].

(This figure is in colour only in the electronic version)

To properly define an event, we set a threshold at SNR $= 4$ and keep only triggers having an SNR $\geqslant 4$. If the time delay between two consecutive triggers above threshold is less than a given time interval (called the clusterization window, set to 10 ms in our analysis), then the triggers are clusterized and considered part of one same event. The time that is then associated with each event corresponds to the time of the trigger, among those of the cluster that defines the event itself, at which the SNR reaches its maximum value. The time duration of the event is given by the time difference between the first and last triggers of the cluster.

[32] recently performed a search for a burst of GWs in coincidence with the long GRB 030329 on data from the LIGO second science run (S2). In figure 2, we compare the Virgo sensitivity curve during C7 with the typical LIGO Hanford sensitivity during the S2. At the time of GRB 030329 both Hanford detectors were taking data, so the cross-correlation between these two detectors was used as the basis of the search algorithm. Our search is instead a single detector approach, based on data from the Virgo detector only. However, we share with this previous analysis some of its basic choices, as the on-source window duration (180 s) and the type of simulated signals used to calibrate the analysis (see section 4.1). Triggered searches using data from single detectors were recently performed in coincidence with the soft gamma-ray repeater SGR 1806-20 [46, 47]. While we work in the time domain and only the trigger-time information is used to define the GRB region, [46] and [47] define time-frequency on-source segments, where the frequency information on the quasi-periodic oscillations (QPOs) observed in the pulsating tail of the giant flare is also taken into account. In the SGR case, this is possible since the target of the coincidence search is the GW emission by the star's seismic modes that, excited in the starquake generating the giant flare, are thought to drive the QPOs.

4.1. The background region

The statistical properties of false alarms are characterized by running the WDF on the *background region*. From the resulting distribution of events versus SNR threshold, we

find that the false alarm rate for SNR > 26 is 5×10^{-4} Hz (see [15] for details), or $\sim$10% false alarm probability in 180 s *assuming Poisson statistics*. As a preliminary choice, we assume SNR $= 26$ as the *threshold*: when scanning the signal region in search for a GW burst coincident with the GRB, we discard all events with SNR lower than 26.

After selecting a threshold, we calibrate our pipeline using software simulations of different waveform types, such as Gaussian, sine-Gaussian and damped sinusoid. In the absence of precise predictions about the waveforms, a Gaussian waveform is representative of generic broadband burst signals; a damped sinusoid could mimic a BH ring-down, expected to have a role in the process of BH formation from a GRB progenitor [12]; finally, a sine-Gaussian could mimic the very last stages of the coalescence process of two compact objects (see, e.g., [48]), as blobs generated by fragmentation instabilities developing in the collapsing core or in the process of disk accretion. Since we expect to be observing the GRB on-axis, i.e. along the rotational axis of its collapsar-type progenitor, considering quadrupolar GW emission from a triaxial ellipsoid rotating about the same axis as the GRB, we would expect the GW signal to be circularly polarized in our direction. Thus, we make the assumption of circular polarization when simulating the waveforms. Moreover, we consider the specific position of GRB 050915a to account for the beam pattern attenuation, which results in $F_+ = 0.32$ and $F_\times = 0.21$ (for a null polarization angle).

The calibration procedure is performed in two main steps. (i) We characterize the filter efficiency in detecting signals at specific frequencies and with specific durations, as a function of their strength. To this end, we consider a simulated burst detected by the filter if an event is found within $\pm$20 ms of the simulated peak time. The preliminary results of this first step of the calibration procedure show that the filter has a detection efficiency $\geqslant$90% for signals above our SNR threshold of 26. (ii) For each simulated waveform, we define a conversion factor between the detected event strength (SNR) and true event strength, which we can characterize in terms of $h_{\rm rss}$, where $h_{\rm rss} = \sqrt{\int_{-\infty}^{+\infty} |h(t)|^2 \, \mathrm{d}t}$ is the 'root-sum-square' amplitude.

4.2. The signal region

Next, we scan the *signal region*. No events are found with SNR > 26, thus we proceed to set an upper limit on the strain amplitude. Assuming SNR $= 26$ as the threshold for a detection, our non-detection upper-limit strain amplitude will correspond, for each type of simulated burst signal, to the $h_{\rm rss}$ value giving a detected SNR of 26.

To have an order of magnitude estimate of the type of upper-limits we are going to set with our analysis, consider, e.g., a signal with central frequency $f_0 \sim 200$ Hz. The mean Virgo strain sensitivity around $\sim$200 Hz was $S_h \sim 6 \times 10^{-22}$ Hz$^{-0.5}$. In the hypothesis of circular polarization, we expect the signal $h_{\rm rss}$ being attenuated for a factor of $\sqrt{\frac{(F_+^2+F_\times^2)}{2}} \sim 0.27$. Thus, in order for the injected signal to be observed at SNR $= 26$, its $h_{\rm rss}$ should be of the order of

$$h_{\rm rss} = 26 \times (6 \times 10^{-22}) \times (0.27)^{-1} \ \mathrm{Hz}^{-1/2} \sim 6 \times 10^{-20} \ \mathrm{Hz}^{-1/2}. \tag{1}$$

The present results of the analysis actually in progress indeed confirm that this is the kind of upper-limit we expect, e.g., for a sine-Gaussian waveform with $Q = 5$ and central frequency $f_0 = 203$ Hz detected with SNR $= 26$.

The final results of our analysis for different waveform types, signal durations and frequencies will be presented in detail in a forthcoming paper [15], where we will also account for the statistical and systematic errors involved in the analysis. The reader is thus referred to this paper for the final results and comparison with other recent coincidence searches [32, 46, 47].

5. Conclusions and future developments

We have given an overview of the present status of an analysis that is being performed on Virgo C7-run data, regarding the search for a burst of GWs associated with the long GRB 050915a. Virgo sensitivity during C7 was comparable to the LIGO sensitivity at the time of its second science run, when a search for a burst of GWs in coincidence with GRB 030329 was performed. This is the first time an analysis of this kind has been performed on Virgo data [14]; thus its final outcome (see [15]) will be a prototype for future similar analyses, which will be carried out taking advantage of the expected improvement in sensitivity.

The case of GRB 070219a, detected by *Swift* [49] during one of the Virgo 'Weekly Science Runs' (WSR9, February 2007), when the sensitivity improved by about a factor of 3 with respect to C7, is currently being analyzed with the same procedure presented here, while another five GRBs were triggered during the current Virgo Science Run (VSR1). For VSR1 data, in view of the possibility of having a joint search with the LIGO detector, the most powerful method for the GRB analysis will be that of the coherent combination of the output of all detectors, which will take advantage of knowledge of the electromagnetic trigger. In a coherent analysis, some basic aspects of the method presented here will certainly be kept, e.g., the use of the WDF, the choice of the on-source data segment, the procedure of pipeline efficiency evaluation for different simulated signals. Moreover, we foresee that a standard coincidence approach, based on this prototype study, will continue to run in parallel with the coherent analysis. The coincidence approach in fact has the advantage of being usually more robust against possible non-stationarities. The case of GRB 050915a, thus, represents a basis for further development of these kinds of studies with Virgo.

References

[1] Costa E *et al* 1997 *Nature* **387** 783
[2] Gehrels N *et al* 2005 *Nature* **437** 851
[3] van Paradijs J *et al* 1997 *Nature* **386** 686
[4] Galama T J *et al* 1998 *Nature* **395** 670
[5] Mészáros P 1999 *Prog. Theor. Phys. Suppl.* **136** 300
[6] Mészáros P 2006 *Rep. Prog. Phys.* **69** 2259
[7] Piran T 1999 *PhR.* **314** 575
[8] Piran T 2005 *Rev. Mod. Phys.* **76** 1143
[9] Meszaros P 2000 *Nu. Ph. S.* **80** 63
[10] van Paradijs J, Kouveliotou C and Wijers R 2000 *Annu. Rev. Astron. Astrophys.* **38** 379
[11] Harrison F 2002 *APS meeting* APR:Y2.003
[12] Kobayashi S and Mészáros P 2003 *Astrophys. J.* **589** 861
[13] http://www.astro.ku.dk/~pallja/GRBsample.html
[14] Corsi A, Cuoco E, Ricci F and Vicerè A 2007 '*Analysis of GRB 050915a as a prototype for GRB searches with Virgo*', Virgo note VIR-020A-07
[15] Acernese F *et al* 2007, in preparation
[16] Woosley S 1993 *Astrophys. J.* **405** 273
[17] Paczyński B 1998 *Astrophys. J.* **494** L45
[18] Fryer C, Woosley S and Hartmann D 1999 *Astrophys. J.* **526** 152
[19] Bloom J S and Prochaska J X 2006 *AIP Conf. Proc.* **836** 473
[20] Hjorth J *et al* 2003 *Nature* **423** 847
[21] Pian E *et al* 2006 *Nature* **442** 1011
[22] Berger E 2006 *AIP Conf. Proc.* **836** 33
[23] Goodman J 1986 *Astrophys. J.* **308** L47
[24] Paczyński B 1986 *Astrophys. J.* **308** L43
[25] Eichler D, Livio M, Piran T and Schramm D 1989 *Nature* **340** 126
[26] Mészáros P and Rees M J 1992 *Astrophys. J.* **397** 570

[27] Mészáros P and Rees M J 1997 *Astrophys. J.* **482** L29
[28] Lee W H and Kluźniak W L 1999 *Astrophys. J.* **526** 178
[29] Rosswog S and Ramirez-Ruiz E 2003 *Mon. Not. R. Astron. Soc.* **343** L36
[30] Rosswog S, Ramirez-Ruiz E and Davies M B 2003 *Mon. Not. R. Astron. Soc.* **345** 1077
[31] Lee W H, Ramirez-Ruiz E and Page D 2004 *Astrophys. J.* **608** L5
[32] Abbott B *et al* 2005 *Phys. Rev.* D **72** 042002
[33] Putten M H *et al* 2004 *Phys. Rev.* D **69** 044007
[34] Gehrels N *et al* 2004 *Astrophys. J.* **611** 1005
[35] Grupe D *et al* 2005 *GRB Coordinates Network* 3977
[36] Barthelmy S *et al* 2005 *GRB Coordinates Network* 3982
[37] Grupe D *et al* 2005 *GRB Coordinates Network* 3983
[38] http://www.virgo.infn.it
[39] Acernese F *et al* 2007 The status of Virgo detector *Class. Quantum Grav.* **24** S381
[40] http://gcn.gsfc.nasa.gov/swift2005_grbs.html
[41] Zhang B and Mészáros P 2004 *Int. J. Mod. Phys.* A **19** 2385
[42] Cuoco E 2005 Wavelet de-noising strategy for transient waveforms identification *VIR-NOT-EGO-1390-305*
[43] Cuoco E 2005 A new wavelet-based method for transients detection. Efficiency with respect whitening algorithms *VIR-NOT-EGO-1390-308*
[44] Cuoco E *et al* 2001 *Class. Quantum. Grav.* **18** 1727
[45] http://www.ligo.caltech.edu/∼jzweizig/distribution/LSC_Data/
[46] Baggio L *et al* 2005 *Phys. Rev. Lett.* **95** 081103
[47] Abbott B *et al* 2007 *Preprint* astro-ph/0703419 (submitted to *Phys. Rev.* D)
[48] Zhuge X, Centrella J M and McMillan S L W 1994 *Phys. Rev.* D **50** 6247
[49] Sakamoto T *et al* 2007 *GRB Coordinates Network* 6104